J Fluor Chem 2014 57 Kravtsov Fonari

Data · April 2014

7 authors, including:

Eduard V. Ganin
Odessa State Environmental University
209 PUBLICATIONS   828 CITATIONS

SEE PROFILE

Marina S Fonari
Institute of Applied Physics Academy of Sciences of R. Moldova
250 PUBLICATIONS   1,462 CITATIONS

SEE PROFILE

Some of the authors of this publication are also working on these related projects:

Metal-organic frameworks View project

Special Edition of Molecules View project

Preparation, structure and properties of pyridinium/bipyridinium hexafluorosilicates

Vladimir O. Gelmboldt [a], Eduard V. Ganin [b], Mark M. Botoshansky [c], Vladimir Yu. Anisimov [a], Olga V. Prodan [a], Victor Ch. Kravtsov [d], Marina S. Fonari [d],*

[a] Odessa National Medical University, Valikhovskiy lane 2, 65026 Odessa, Ukraine
[b] Odessa State Environmental University, Lvovskaya Str. 15, 65016 Odessa, Ukraine
[c] Schulich Faculty of Chemistry, Technion-Israel Institute of Technology, Technion City, 32000 Haifa, Israel
[d] Institute of Applied Physics, Academy of Sciences of Moldova, Academy Str. 5, MD2028 Chisinau, Republic of Moldova

A B S T R A C T

Pyridinium hexafluorosilicates with the compositions $(LH)_2[SiF_6]$ (where L = 2,6-bis(hydroxymethyl)-pyridine (**I**), 4,5-bis(hydroxymethyl)-2-methylpyridine-3-ol (**II**)), monohydrate $(LH)_2[SiF_6]\cdot H_2O$ (L = 2-bromo-6-methylpyridine (**III**)) and $(LH_2)[SiF_6]$ (L = 4,4′-bipyridine (**IV**), 2,2′-bipyridine (**V**)) were separated as crystalline products of interaction of fluorosilicic acid with different pyridines. All compounds were characterized by elemental analysis, IR, NMR ^{19}F and mass-spectrometry, solubility data, and X-ray crystallography. The structural study revealed the details of the anion binding and solid state supramolecular architectures provided by the combination of the plethora of intermolecular interactions including strong charge assisted and conventional hydrogen bonds of NH···F, OH···F types along with O···Br contacts and π–π interactions. The relationship between the salts structure and physico-chemical properties is discussed.

© 2014 Elsevier B.V. All rights reserved.

1. Introduction

Fluorosilicic acid, the large-capacity by-product in production of phosphate fertilizers and elemental phosphorus, is considered as a main alternative source of fluorine for chemical industry [1]. One of the existing ways of utilization of fluorosilicic acid is its use for the fluoridation of drinking water (in the U.S., the UK and Ireland) to prevent the dental caries disease [2,3]. In their turn, the "onium" hexafluorosilicates, in particular, ammonium hexafluorosilicate (AHF) $(NH_4)_2[SiF_6]$ and hexafluorosilicates of amino acids represent in the recent years the objects of intensive research as compounds possessing by the caries-protected and hyposensitive properties [4–10].

Nowadays AHF is proposed as a possible alternative to the known drug silver diamine fluoride, $[Ag(NH_3)_2]F$ [11], which, having an effective remineralizing and bactericidal action, causes an undesirable darkening of the treated hard dental tissues. Otherwise, AHF being deprived of this drawback has a number of advantages. In particular, according to [4,12] silica, as a product of hydrolysis of AHF, acts as a non-trivial catalyst promoting the

deposition of calcium phosphate or fluorapatite from saliva and similar biological liquids; silica is present in sediment that is formed on the dentin surface [4], thus providing prolonged dentin tubule occlusion. On another hand one more positive aspect of AHF is an increased acid resistance of both tooth enamel and dentin [13]. It is supposed that the other "onium" hexafluorosilicates, for example, with heterocyclic cations must have similar effect. For example, the patented data [14] suggested the hexafluorosilicates of benzyl ester of 3-pyridincarbonic acid and monoalkylammonium $(C_{12}–C_{18})$ as caries-protected agents.

However, the physico-chemical properties of hexafluorosilicates as potential caries protectors are studied insufficiently. Recently we reported the aqueous solubility data for carboxypyridinium and aminopyridinium hexafluorosilicates [15,16]. This contribution continues that study and covers the synthesis, structure and properties of several substituted pyridinium hexafluorosilicates with the compositions $(LH)_2[SiF_6]$ (where L = 2,6-bis(hydroxymethyl)pyridine (**I**), 4,5-bis(hydroxymethyl)-2-methylpyridine-3-ol (**II**)), monohydrate $(LH)_2[SiF_6]\cdot H_2O$ (L = 2-bromo-6-methylpyridine (**III**)) and $(LH_2)[SiF_6]$ (L = 4,4′-bipyridine (**IV**), 2,2′-bipyridine (**V**)). According to the reported calculated data [17] the specific feature of all selected ligands is their high probability for saliva stimulation. This factor is of undoubted interest in the context of the potential use of the corresponding hexafluorosilicates in the dental practice.

* Corresponding author. Tel.: +373 22738154; fax: +373 22725887.
  E-mail addresses: fonari.xray@phys.asm.md, fonari.xray@gmail.com
(M.S. Fonari).

Table 1
Crystal data and structure refinement for **I–V**, **Vb**.

Identification code	I	II	III	IV	V	Vb
Empirical formula	$(C_{14}H_{20}N_2O_4)[SiF_6]$	$(C_{16}H_{24}N_2O_6)[SiF_6]$	$(C_{12}H_{18}Br_2N_2O_2)[SiF_6]$	$(C_{10}H_{10}N_2)[SiF_6]$	$(C_{10}H_{10}N_2)[SiF_6]$	$(C_{10}H_8N_2)[SiF_4]$
Formula weight	422.41	482.46	524.19	300.29	300.29	260.27
Crystal system	monoclinic	monoclinic	triclinic	orthorhombic	monoclinic	monoclinic
Space group	C2/m	C2/c	P-1	Pbcn	I2/a	P2₁/n
Unit cell dimensions						
a (Å)	6.7516(6)	17.541(3)	7.075(1)	11.897(2)	12.396(4)	7.1895(2)
b (Å)	12.6150(8)	13.3306(18)	8.187(2)	7.188(2)	6.6042(7)	9.1687(4)
c (Å)	9.9183(7)	9.3848(18)	8.542(2)	12.882(3)	13.475(3)	16.2498(5)
α (°)	90	90	72.05(2)	90	90	90
β (°)	101.286(7)	115.71(2)	80.18(2)	90	92.46(4)	98.185(3)
γ (°)	90	90	73.42(2)	90	90	90
Volume (Å³)	828.42(11)	1977.2(6)	449.27(16)	1101.6(4)	1102.1(5)	1060.24(7)
Z	2	4	1	4	4	4
D (calcd) (Mg/m³)	1.693	1.621	1.937	1.811	1.810	1.631
μ (mm⁻¹)	0.232	0.213	4.646	0.283	0.283	0.255
F(000)	436	1000	258	608	608	528
Reflections collected	1417	3251	5249	3038	1908	4020
Independent reflections	810 [R(int) = 0.0242]	3251 [R(int) = N/A]	1436 [R(int) = 0.0958]	938 [R(int) = 0.0475]	972 [R(int) = 0.0254]	1973 [R(int) = 0.0273]
Data/restraints/parameters	810/0/77	3251/4/164	1436/3/122	938/0/92	972/0/91	1973/0/154
Goodness-of-fit on F2	1.011	0.985	1.126	0.912	1.074	1.060
Final R indices [I > 2σ(I)], R₁, wR₂	0.0420, 0.0965	0.0440, 0.0886	0.0944, 0.2434	0.0332, 0.0886	0.0423, 0.0999	0.0425, 0.0988
R indices (all data) R₁, wR₂	0.0579, 0.1113	0.0919, 0.1028	0.1069, 0.2639	0.0488, 0.0960	0.0579, 0.1151	0.0601, 0.1111
Largest diff. peak and hole (e Å−3)	0.208 and −0.300	0.218 and −0.318	1.597 and −1.432	0.261 and −0.211	0.306 and −0.332	0.169 and −0.299

2. Results and discussion

2.1. Crystal structures

All compounds were obtained by interaction of relevant *N*-base with fluorosilicic acid in aqueous solution. Crystal structure and refinement data for **I–V** and unexpected product **Vb** are given in Table 1, hydrogen bonding geometry is summarized in Table 2. Six structures can be naturally separated into two groups, the first one based on pyridine derivatives includes complexes **I–III**, and the second one based on bipyridine derivatives includes complexes **IV**, **V**, and **Vb**. Their formula units are shown in Fig. 1. Compounds **I–III** have the 1:2 acid:base ratio with the $[SiF_6]^{2-}$ anion occupying position on inversion centers in the centrosymmetric C2/m (**I**), C2/c (**II**), and P-1 (**III**) space groups. Compounds **IV** and **V** also crystallize in the centrosymmetric orthorhombic Pbcn and monoclinic I2/a space groups. They have the 1:1 acid:base ratio with the $[SiF_6]^{2-}$ anion occupying position on inversion centers again, and bipyridinium ligands residing on the two-fold axes that cross

the middle of single C–C bonds in the dications. The detailed inspection of crystalline product **V** revealed that this material is composed of two types of crystals, the major component being an expected salt (LH₂)[SiF₆] **V**, and the minor component being unexpected chelate cis-[SiF₄(2,2′-Bipy)] (2,2′-Bipy = 2,2′-bipyridine) (**Vb**) (Fig. 1f) previously reported in [18]. The positions of *N*-bound hydrogen atoms were found in the difference Fourier map. Proton transfer to the pyridine nitrogen atom is clearly indicated by the widened C–N–C bond angles in the aromatic rings falling in the range 122.2(2)–124.2(3)°. Hexafluorosilicate anion in the structures has the geometry of the distorted octahedron with the Si–F distances running from 1.658(2) till 1.706(2) Å. The ionic species are held together via strong charge-assisted NH⁺···F⁻ hydrogen bonds (Table 2).

As the single crystal X-ray structural analysis revealed, the correlation repeatedly marked in the literature [19] works for the majority of the structures reported herein, namely, in **I, II, IV, V** the longest Si–F covalent bonds correspond to the fluorine atoms involved in the strongest XH···F (X = N, O) hydrogen bonds, the

Table 2
Hydrogen bonds for **I–V** [Å and °].

| D–H···A	d(H···A)	d(D···A)	∠(DHA)	Symmetry transformation for acceptor
I				
N(1)–H(1N)···F(3)	1.82(4)	2.737(3)	166(4)	x, y, z
O(1)–H(1O1)···F(1)	2.10(4)	2.968(2)	162(3)	x + 1/2, y + 1/2, z
O(1)–H(1O1)···F(2)	2.30(4)	2.987(2)	133(3)	x + 1/2, y + 1/2, z
II				
O(1)–H(1)···O(2)	1.66(2)	2.483(2)	160(3)	x, y, z
O(2)–H(2)···F(2)	1.84(2)	2.633(3)	147(3)	2 − x, y, 3/2 − z
O(3)–H(3)···F(1)	1.95(2)	2.757(2)	165(3)	3/2 − x, y + 1/2, 3/2 − z
O(3)–H(3)···F(3)	2.52(3)	3.092(3)	127(3)	x, y, z
N(1)–H(1N)···F(3)	1.83(2)	2.707(3)	171(2)	x, y, z
N(1)–H(1N)···F(1)	2.55(2)	3.052(2)	117(2)	3/2 − x, 1/2 − y, 2 − z
III				
O(1W)–H(1A)···F(1)	1.98(4)	2.803(8)	161(10)	x, y, z
O(1W)–H(1B)···F(3)	1.96(4)	2.782(7)	160(11)	x + 1, y, z
N(1)–H(1)···O(1W)	1.85	2.709(9)	174	x, y, z
IV				
N(1)–H(1N)···F(3)	1.82(3)	2.695(2)	159(2)	x, y, z
V				
N(1)–H(1N)···F(3)	1.77(3)	2.711(3)	179(3)	x, y, z
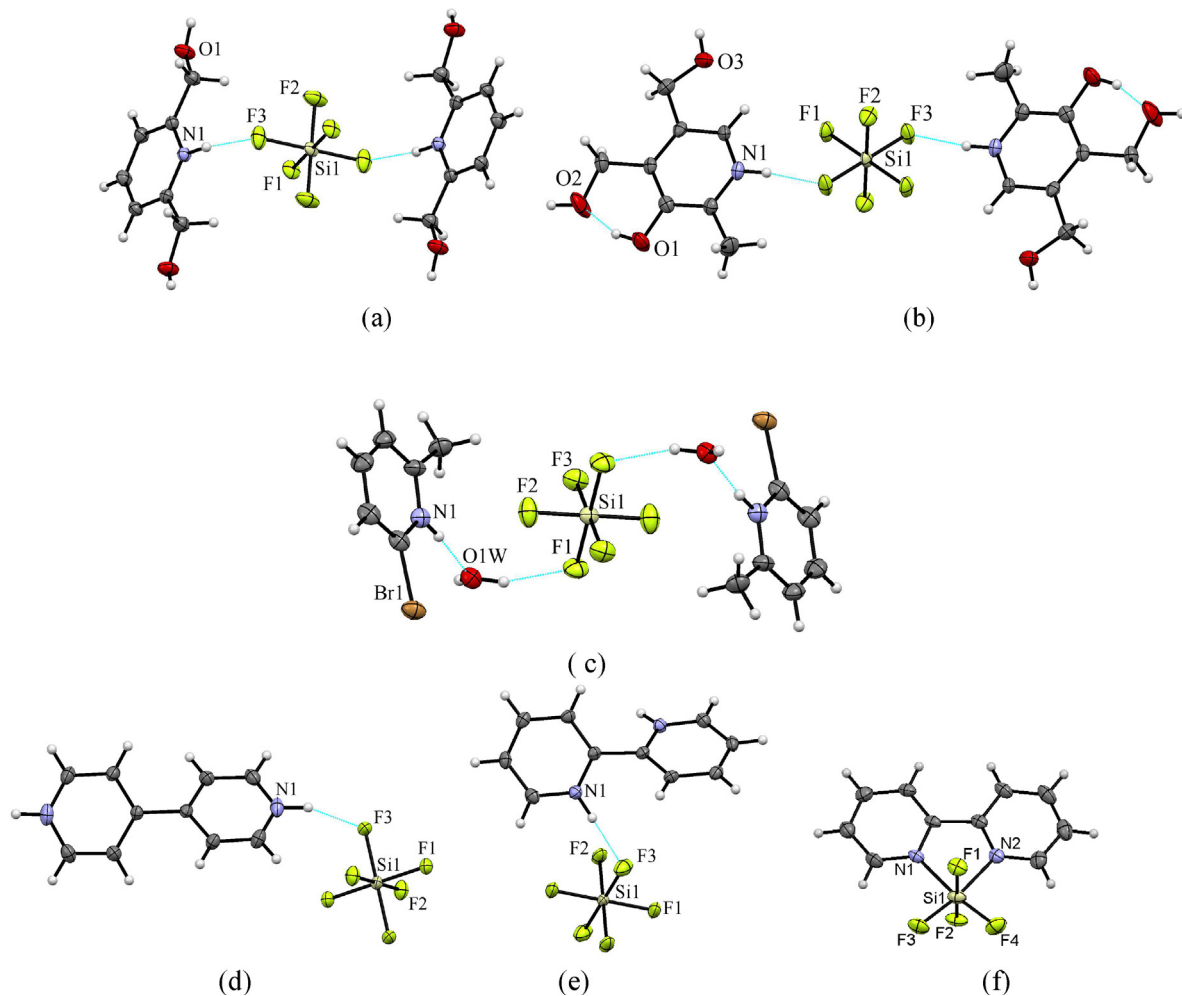
Fig. 1. ORTEP drawings for formula units in **I–V**, **Vb** with partial labeling scheme.

shortest Si–F bonds found for fluorine atoms not involved in H-bonds. The most clearly this tendency is unclosed for complexes **IV** and **V**, with one strong N(1)H$\cdots$F(3) hydrogen bond (Fig. 1d and e); the Si–F(3) bond distances being 1.7052(19) and 1,7054(10) Å and considerably exceed the Si–F(1) and Si–F(2) bond distances for fluorine atoms not involved in the H– bonding (1.6637(16)–1.6750(11) Å).

The additional H-donor centers in **I** and **II**, the incorporation of water molecule and Br$\cdots$O contacts in **III**, and numerous CH$\cdots$F short contacts and stacking interactions in **IV** and **V** also specify the supramolecular architecture of these compounds. The solid **I** represents the layered structure. The H-bonded layer may be interpreted as composed of two interpenetrated H-bonded arrays, the three-membered formula units held by a couple of NH$^+\cdots$F$^-$ hydrogen bonds (Fig. 1a), and combination of acentric $R_1^2(3)$ and centrosymmetric $R_4^2(20)$ patterns [20] with the involvement of hydroxyl oxygens and four other fluorines of anions affording infinitive tapes running along the b direction (Fig. 2a). The C_{2v} molecular symmetry of 2,6-bis(hydroxymethyl)pyridine in **I** provides the symmetric layer developed parallel to the ab plane (Fig. 2b). The layer thickness equals to $c\cdot\sin\beta = 9.727$ Å (Fig. 2b). The difference in positions and number of hydroxyl groups in 4,5-bis(hydroxymethyl)-2-methylpyridine-3-ol in **II** resulted in rearrangement of hydrogen bonding patterns, that represent now the interpenetration of two 1D infinitive motifs built of the different $R_4^4(20)$ and $R_4^4(20)$ H-bonded patterns (Fig. 3a and b) acting similar to **I** within the double layer developed parallel to the (0 1 1) crystallographic plane, the layer thickness being of

$1/2a\cdot\sin\beta = 7.902$ Å in **II**, the interlayer interaction is supported with strong O2$\cdots$F2 H-bond (Table 2) that combines the layers into 3D network along the a axis (Fig. 3c).

In structure **III** the hydrogen bonds unite the structural components in linear motif (Fig. 4). The water molecules act as double H-donors toward the successive [SiF$_6$]$^{2-}$ anions with the formation of the centrosymmetric $R_4^4(12)$ H-bonded patterns that combine two water molecules and two [SiF$_6$]$^{2-}$ anions, giving rise to the infinite chain running along the a direction in the unit cell. Moreover, water molecules act as acceptor toward the NH-site in pyridinium cations, which decorate the chain. Infinite stacking interactions between pyridinium cations along the a axis unite chains in layers parallel to the (0 1 1) crystallographic plane. The interplanar distances between the parallel aromatic moieties in the stack equal to 3.409 and 3.425 Å, and corresponding centroid$\cdots$centroid separations being 3.718 and 3.972 Å. The short O$\cdots$Br contacts of 2.975 Å and CH$\cdots$F interactions unite the layers in 3D network.

In the solids **IV** and **V** the charged components alternate in the chains, being linear in **IV** and meander-like ones in **V** (Fig. 5a and b). The components are held together *via* NH$\cdots$F hydrogen bonds. Both 2,2′ and 4,4′-bipyridinium dications have the twisted shapes with the dihedral angles between the aromatic rings of 44.3° in **IV** and 36.4° in **V**. In both structures the tapes stack along the c directions with the alternation of hydrophilic and hydrophobic regions.

The contribution of weaker CH$\cdots$F hydrogen bonding which as one of the major factors for stabilization of these two solids should
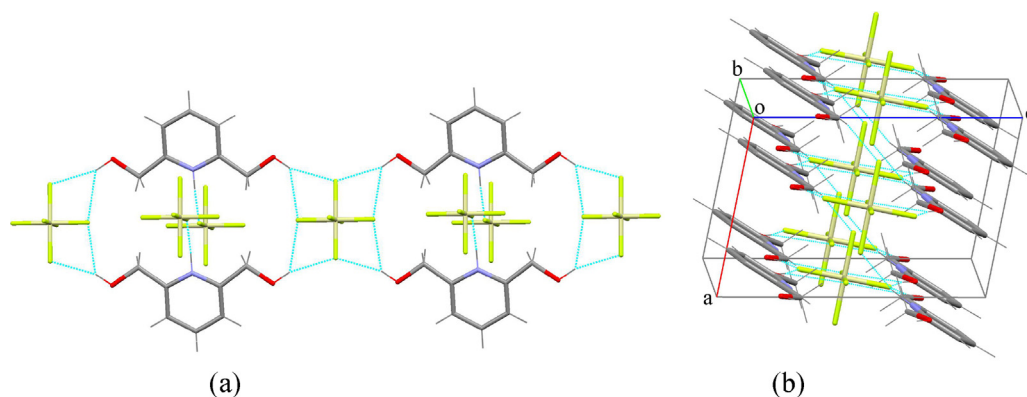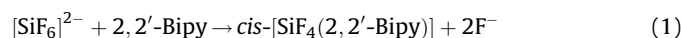
Fig. 2. Packing motifs in **I**. (a) 1D array developed along the *b* direction. (b) Side view of H-bonded layer.

be mentioned here as far as all C-bound H-atoms are involved in short CH···F contacts in **IV**, H···F and C···F being in the range 2.41–2.51 and 3.176–3.394 Å, and all but one CH-groups are involved in the short H···F contacts in **V**, H···F and C···F being in the range 2.38–2.43 and 3.007–3.281 Å. The importance of CH···F bonding has been recently declared for the hexafluorosilicates of closely related heterocyclic bases [21–23]. For example, it might be noted that bis(1-methyl-3-propylimidazolium) hexafluorosilicate, [Pmim]$_2$[SiF$_6$] has appeared to be unsuccessful candidate for ionic liquid (this salt has high melting point, 210 °C) primarily due to structure stabilization by very short CH···F contacts, 1.94–2.42 Å [21]. Somewhat similar situation occurs in the case of related 4,4′-bipyrazolium hexafluorosilicate, [H$_2$bpz][SiF$_6$] stabilized, along with strong NH···F hydrogen bonds also by weaker CH···F contacts [22]. Bis-pyridazine tectons support the structure of metallosupramolecular cavitand Cu$_2$L$_4$$^{4+}$, which is capable of selective encapsulation of [SiF$_6$]$^{2-}$ anions by a concerted action of two coordination and twelve CH···F bonds [23].

The most intriguing result reported herein is the detection and structural identification of the chelate complex *cis*-[SiF$_4$(2,2′-Bipy)] (**Vb**) as one of the products of fluorosilicic acid interaction with

2,2′-Bipy. It is known that the silicon tetrafluoride complexes with *N*-donor ligands reveal extremely low hydrolytic stability, therefore their synthesis by interaction of SiF$_4$ with ligands is carried out in anhydrous solvents or in gas phase [24]. Even in the humid air complexes tend to be converted into the corresponding hexafluorosilicates. Evidently, the detection of complex **Vb** as a by-product of **V** crystallized from aqueous solution, is provided by the chelating ligand effect, according to scheme (1). Compound **Vb** represents the first structurally confirmed example of molecular complex formed by SiF$_4$ with *N*-donor ligand separated from the mixed aqueous-organic medium, which retains its structure after recrystallization from aqueous solution.

$$[SiF_6]^{2-} + 2, 2'\text{-Bipy} \rightarrow cis\text{-}[SiF_4(2, 2'\text{-Bipy})] + 2F^- \qquad (1)$$

2.2. Selected physico-chemical properties

2.2.1. Solubility in water

It has been previously shown [16] that for the substituted pyridinium hexafluorosilicates their water solubility correlates
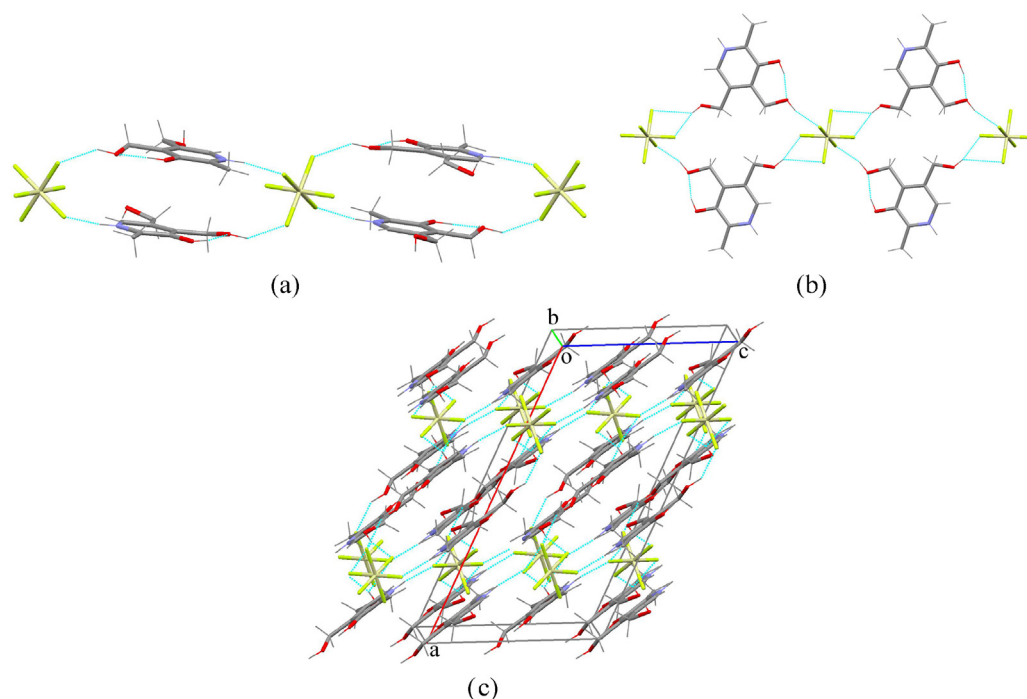

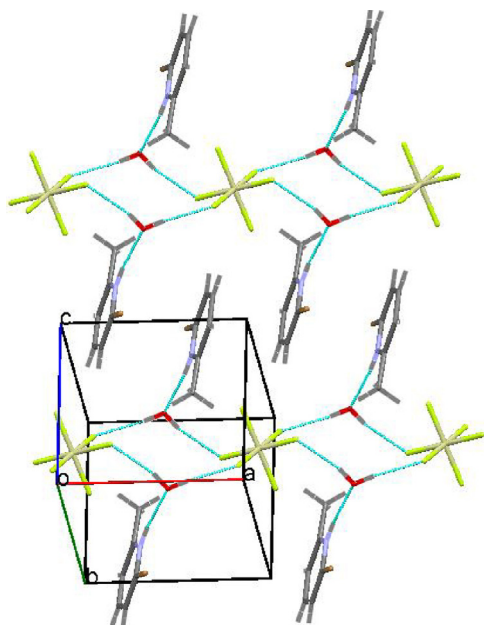**Fig. 3.** Packing motifs in **II**. (a and b) 1D arrays. (c) 3D network.

Fig. 4. Packing motifs in **III**.
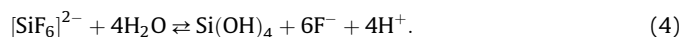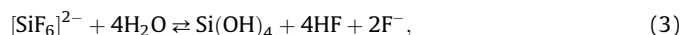
with parameter h defined as

$$h = \frac{n}{d(D \cdots A)_{av.}}, \qquad (2)$$

where n is the number of short inter-ionic contacts (that include strong and medium H-bonds, $D \cdots A \leq 3.2$ Å [25]), $d(D \cdots A)_{av.}$ is an average donor-acceptor distance in the complex structure. The increase in h values means an increase in intensity of inter-ionic H-bond interactions, and results in an exponential decrease of solubility of the relevant hexafluorosilicates. Table 3 summarizes the solubility data for the newly synthesized salts **I–V** together with the previously reported hexafluorosilicates, and the numerical values for parameter h calculated from the X-ray data. In concordance with the data reported in [15,16] the pyridinium salts **I–III** reveal the tendency toward solubility decrease with increase the number of H-donors in the pyridinium moieties. Thus, the decrease in solubility for compounds **I** and **II** in comparison with 2-methyl- and 2,6-dimethylpyridinium hexafluorosilicates is associated with the presence of OH-donor groups in the pyridinium cations. The similar effect observed for monohydrate **III** is explained by the same reason, as far as the water inclusion

provides an additional stabilization of salt due to the extended system of H-bonds (increase of parameter h) (Table 3) [27]. However, the observed significant difference (in order of magnitude) in water solubility for the salts of isomeric dipyridinium cations **IV** and **V**, which are characterized by the same h value, cannot be resolved within the framework of this concept, and probably is explained by structural factors unaccounted in [16]. It is noteworthy that the solubility data for compound **II** illustrate the so-called Lipinski "rule of 5" [28] that predicts the low water solubility and absorption for compounds with the number of H-donors $N_H > 5$.

2.2.2. Hydrolysis

It is known [2] that in aqueous solutions the hexafluorosilicates are subjected to hydrolytic transformations with the formation of hydrated form of silica (silicic acid), and hydrofluoric acid (fluoride ions) in accordance with the general schemes:

$$[SiF_6]^{2-} + 4H_2O \rightleftharpoons Si(OH)_4 + 4HF + 2F^-, \qquad (3)$$

$$[SiF_6]^{2-} + 4H_2O \rightleftharpoons Si(OH)_4 + 6F^- + 4H^+. \qquad (4)$$

The hydrolysis process is generally controlled by ^{19}F NMR spectrometry and pH-measurements [2,26,29]. The formation of silica is registered by spectral tests [29]. As it has been above noted, the silicic acid as a hydrolytic product is an essential component providing caries-protected and hyposensitive action of AHF. In this regard, particular interest represents the comparative evaluation of the degree of hydrolysis for pyridinium/bipyridinium hexafluorosilicates and AHF. Table 4 shows the results of determining the degree of hydrolysis for hexafluorosilicates in 1×10^{-4} M aqueous solutions. The degree of hydrolysis for compound **V** could not be determined in spite of the expected development of the yellow color of the reaction solution after addition of $(NH_4)_2MoO_4$, as far as its intense opalescence impedes the spectrophotometric measurements.

As it follows from the reported data, the degree of hydrolysis for all studied hexafluorosilicates is consistently high, reaching in some cases almost quantitative values. High degree of conversion of $[SiF_6]^{2-}$ anions into silicic acid (silica) in dilute aqueous solutions facilitates, according to schemes (3) and (4) an effective release of fluoride ions, that together with formation of silica, should provide caries-protected effect of studied compounds. It should be noted that we did not register in the ^{19}F NMR spectra of aqueous solutions **I–V** the signals of any intermediate products of
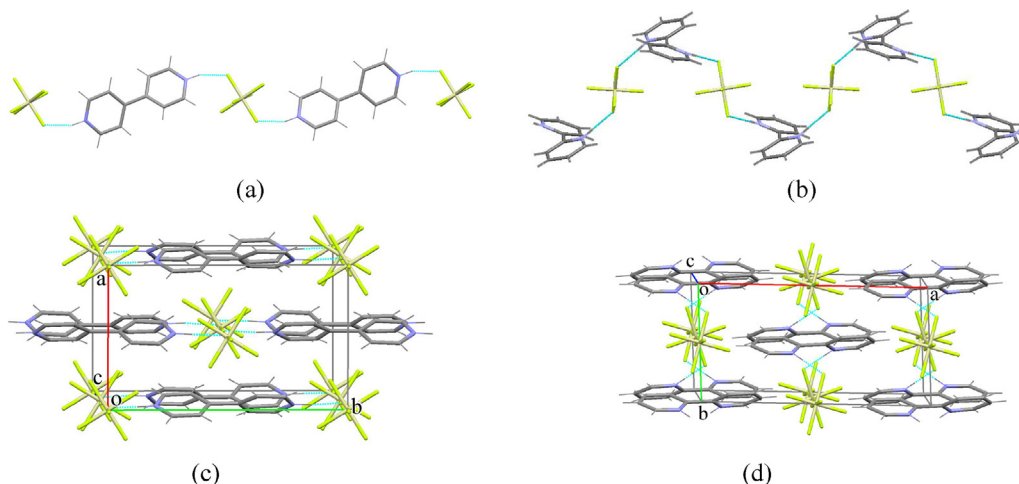

(a)

(b)

(c)

(d)

Fig. 5. Packing motifs in **IV** and **V**. (a) side view of the linear chains in **IV**; (b) side view of the meander-like chain in **V**; (c) packing of chains in **IV**; (d) packing of chains in **V**.

Table 3
Solubility of pyridinium hexafluorosilicates in water and h values.

Compound	Solubility (mol. %, 25 °C)	h (Å^{-1})
[2-CH$_3$C$_5$H$_3$NH]$_2$[SiF$_6$]	11.60[a]	0.71 [26]
[2,6-(CH$_3$)$_2$C$_5$H$_3$NH]$_2$[SiF$_6$]	9.90	0.72 [26]
[2-HO(O)CC$_5$H$_4$NH]$_2$[SiF$_6$]	5.33[a]	0.76 [16]
[3-HO(O)CC$_5$H$_4$NH]$_2$[SiF$_6$]	3.33[a]	1.09 [16]
[2,6-(HOCH$_2$)$_2$C$_5$H$_3$NH]$_2$[SiF$_6$]	2.52	1.04
[2-CH$_3$-3-OH-4,5-(HOCH$_2$)$_2$C$_5$HNH]$_2$[SiF$_6$]	0.89	1.68
[2-Br-6-CH$_3$C$_5$H$_3$NH]$_2$[SiF$_6$]·H$_2$O	2.01	1.42
[2,2′-BipyH$_2$][SiF$_6$][b]	10.58	0.37
[4,4′-BipyH$_2$][SiF$_6$]	0.36	0.37

[a] Data from [15].
[b] Contains the admixture of complex *cis*-[SiF$_4$·2,2′-Dipy].

Table 4
Degree of hydrolysis for hexafluorosilicates in 1×10^{-4} M aqueous solutions.

Compound	α (%)
(NH$_4$)$_2$[SiF$_6$]	95.6
[2,6-(HOCH$_2$)$_2$C$_5$H$_3$NH]$_2$[SiF$_6$]	96.7
[2-CH$_3$-3-OH-4,5-(HOCH$_2$)$_2$C$_5$HNH]$_2$[SiF$_6$]	98.0
[2-Br-6-CH$_3$C$_5$H$_3$NH]$_2$[SiF$_6$]·H$_2$O	93.5
[4,4′-BipyH$_2$][SiF$_6$]	94.7

hydrolysis of the [SiF$_6$]$^{2-}$ anion, for example [SiF$_5$·H$_2$O]$^-$, as reported by the authors in [26].

3. Conclusions

Concluding, the products of interaction of fluorosilicic acid with substituted pyridines 2,6-bis(hydroxymethyl)pyridine, 4,5-bis(hydroxymethyl)-2-methylpyridine-3-ol, 2-bromo-6-methylpyridine, and 2,2′- and 4,4′-bipyridines represent expected pyridinium(bipyridinium) hexafluorosilicates. The crystal structures are stabilized by the systems of inter-ionic H-bonds, which provide significant impact on the salts' aqueous solubility, lowering it with increase of H-donors in the corresponding pyridinium cations. For complexes **I** and **II** the involvement of hydroxyl groups in the cation–anion H-binding was demonstrated for the first time. The studied compounds are characterized by the predicted high tendency to hydrolysis in dilute aqueous solutions with the formation of silica and fluoride anion that allows considering these salts as potential caries-protected agents. The study of biological activity of these compounds is the subject of further investigations.

4. Experimental

The IR-absorption spectra were recorded on a spectrophotometer Spectrum BX II FT-IR System (Perkin-Elmer) (range 4000–350 cm^{-1}, samples as tablets with KBr). ^{19}F NMR spectra were recorded on Varian Gemini-200 spectrometer (188.14 MHz, CFCl$_3$ as standard). The mass spectra were registered on a spectrometer MX-1321 (direct input of a sample in a source, energy of ionizing electrons 70 eV). The isothermal conditions of experiments on detection of solubility and degree of hydrolysis of hexafluorosilicates ($t = 25 \pm 0.2$ °C) were provided with the help of an ultra thermostat U15. The determination of the soluble form of silica (orthosilicic acid, formally SiO$_2$·2H$_2$O) in the hydrolyzed hexafluorosilicates was conducted by photocolorimetric method similar to reported in [29], which is based on the ability of silicic acid to form with molybdate ions (reagent – ammonium molybdate, (NH$_4$)$_2$MoO$_4$) in acidic medium the complex silicomolybdic acid as a yellow chromophore. Measurements were performed at 380 nm using a spectrophotometer KFK-3. The degree of hydrolysis α was calculated

by the formula $\alpha = C_{Si, hydr.}/C_{Si, total}$, where the $C_{Si, hydr.}$ – concentration of silicon determined in the hydrolytic products in the form of silicic acid, $C_{Si, total}$ – calculated combined silicon concentration in salt solutions. The commercial ammonium hexafluorosilicate (Sigma–Aldrich) has been used.

4.1. Synthesis of bis[2,6-bis(hydroxymethyl)pyridinium] hexafluorosilicate (**I**)

2,6-Bis(hydroxymethyl)pyridine (L^1; 1.39 g, 0.01 mol) was dissolved in boiling methanol (100 mL) and to the obtained solution the fluorosilicic acid (FSA, 45%, 9 mL, molar ratio L^1:FSA = 1:3) was added. A reaction mixture stored at ambient conditions prior to the beginning of crystallization of the reaction product, which was obtained in an approximately qualitative yield. Colorless transparent crystals with the composition (L^{1}H)$_2$[SiF$_6$] (**I**) with m.p. > 150 °C (with decomposition). Anal. found, %: Si 6.92, N 6.38, F 29.18. Calcd. for C$_{14}$H$_{20}$F$_6$N$_2$O$_4$Si: Si 6.65, N 6.63, F 26.99. Mass spectrum: [ML^1]$^{•+}$ ($m/z = 139$, $I = 22\%$), [ML^1–H]$^+$ ($m/z = 138$, $I = 84\%$), [ML^1–H$_2$O]$^+$ ($m/z = 121$, $I = 30\%$), [SiF$_3$]$^+$ ($m/z = 85$, $I = 100\%$). IR-spectrum: 3315, 3165, 3129 (ν(OH), ν(NH$^+$)), 723 (ν(SiF)), 482 (δ(SiF$_2$)). ^{19}F NMR (188.14 MHz, D$_2$O): $\delta = -130.70$ ppm (s, J(SiF) = 107.6 Hz, SiF$_6$$^{2-}$).

4.2. Synthesis of bis[4,5-bis(hydroxymethyl)-2-methylpyridinium-3-ol] hexafluorosilicate (**II**)

4,5-Bis(hydroxymethyl)-2-methylpyridine-3-ol (L^2; 1.69 g, 0.01 mol) was dissolved in boiling methanol (70 mL) and to the obtained solution the fluorosilicic acid (FSA, 45%, 9 mL, molar ratio L^2:FSA = 1:3) was added. A reaction mixture stored at ambient conditions prior to the beginning of crystallization of the reaction product, which was obtained in an approximately qualitative yield. Colorless transparent crystals of the composition (L^{2}H)$_2$[SiF$_6$] (**II**) with m.p. > 175 °C (with decomposition). Anal. found, %: Si 5.59, N 5.88, F 22.14. Calcd. for C$_{16}$H$_{24}$F$_6$N$_2$O$_6$Si: Si 5.82, N 5.81, F 23.63. Mass spectrum: [ML^2]$^{•+}$ ($m/z = 169$, $I = 53\%$), [ML^2–H$_2$O]$^{•+}$ ($m/z = 151$, $I = 50\%$), [ML^2–H$_2$O–CHO$_2$]$^+$ ($m/z = 106$, $I = 52\%$), [ML^2–H$_2$O–CO–HCO]$^+$ ($m/z = 94$, $I = 100\%$), [SiF$_3$]$^+$ ($m/z = 85$, $I = 67\%$). IR-spectrum: 3350, 3277, 3094 (ν(OH), ν(NH$^+$)), 721 (ν(SiF)), 482 (δ(SiF$_2$)). ^{19}F NMR (188.14 MHz, D$_2$O): $\delta = -130.59$ ppm (s, J(SiF) = 100.2 Hz, SiF$_6$$^{2-}$).

4.3. Synthesis of bis[(2-bromo-6-methylpyridinium)hexafluorosilicate] monohydrate (**III**)

2-Bromo-6-methylpyridine (L^3; 1.72 g, 0.01 mol) was dissolved in boiling methanol (150 mL) and to the obtained solution the fluorosilicic acid (FSA, 45%, 9 mL, molar ratio L^3:FSA = 1:3) was added. A reaction mixture stored at ambient conditions prior to the beginning of crystallization of the reaction product, which was obtained in an approximately qualitative yield. Colorless transparent crystals of the composition (L^{3}H)$_2$[SiF$_6$]·H$_2$O (**III**) with m.p. > 230 °C (with decomposition). Anal. found, %: Si 5.41, N 5.70, F 24.11. Calcd. for C$_{12}$H$_{16}$Br$_2$F$_6$N$_2$OSi: Si 5.55, N 5.53, F 22.52. Mass spectrum: [ML]$^{•+}$ ($m/z = 172$, $I = 39\%$), [SiF$_3$]$^+$ ($m/z = 85$, $I = 100\%$). IR-spectrum: 3391, 3380, 3305, 3218 (ν(OH), ν(NH$^+$)), 733 (ν(SiF)), 485, 425 (δ(SiF$_2$)). ^{19}F NMR (188.14 MHz, D$_2$O): $\delta = -129.31$ ppm (s, SiF$_6$$^{2-}$).

4.4. Synthesis of (4,4′-bipyridinium) hexafluorosilicate (**IV**)

4,4′-Bipyridine (L^4; 1.56 g, 0.01 mol) was dissolved in boiling methanol (100 mL) and to the obtained solution the fluorosilicic acid (FSA, 45%, 9 mL, molar ratio L^3:FSA = 1:3) was added. A reaction mixture stored at ambient conditions prior to the

beginning of crystallization of the reaction product, which was obtained in an approximately qualitative yield. Colorless transparent crystals with the composition $(L^4H_2)[SiF_6]$ (**IV**) with m.p. $> 245\ ^\circ C$ (with decomposition). Anal. found, %: Si 9.12, N 9.51, F 39.24. Calcd. for $C_{10}H_{10}F_6N_2S$: Si 9.35, N 9.33, F 37.96. Mass spectrum: $[ML^4]^{\bullet+}$ ($m/z = 156$, $I = 100\%$), $[ML^4-H_2CN]^+$ ($m/z = 128$, $I = 12\%$), $[SiF_3]^+$ ($m/z = 85$, $I = 45\%$). IR-spectrum: 3441, 3184, 3098 ($\nu(NH^+)$), 720 ($\nu(SiF)$), 482, 436 ($\delta(SiF_2)$). ^{19}F NMR (188.14 MHz, D_2O): $\delta = -130.39$ ppm (s, J(SiF) = 103.6 Hz, SiF_6^{2-}).

4.5. Synthesis of (2,2′-bipyridinium) hexafluorosilicate (V)

2,2′-Bipyridine (L^5; 1.56 g, 0.01 mol) was dissolved in boiling methanol (100 mL) and to the obtained solution the fluorosilicic acid (FSA, 45%, 9 mL, molar ratio L^3:FSA = 1:3) was added. A reaction mixture stored at ambient conditions prior to the beginning of crystallization of the reaction product. The precipitate was recrystallized from water, thus giving rise to the single crystals of two different types. For the dominant (major) crystalline product the elemental analysis was carried out. Colorless transparent crystals with the composition $(L^5H_2)[SiF_6]$ (**V**) with m.p. $>235–240\ ^\circ C$ (with decomposition). Anal. found, %: Si 9.41, N 9.59, F 35.33. Calcd. for $C_{10}H_{10}F_6N_2S$: Si 9.35, N 9.33, F 37.96. ^{19}F NMR (188.14 MHz, D_2O): $\delta = -130.40$ ppm (s, SiF_6^{2-}).

4.6. X-ray structure determination for I–V

The X-ray intensity data for **I**, **II**, **V**, and **Vb** were collected at a room temperature on a Xcalibur E diffractometer, and for **III** and **IV** on Nonius Kappa diffractometer, both equipped with CCD area detectors and a graphite monochromator utilizing MoKα radiation. Final unit cell dimensions were obtained and refined on an entire data set. Lorentz, polarization, and empirical absorption corrections were applied for diffracted reflections. All calculations to solve the structures and to refine the models were carried out with the programs SHELX97 [30]. The structure of **II** was refined as non-merohedral two-component twin. The twin components were resolved using CrysAlisPro software, version 1.171.35.21b, the twin matrix for the second component (0.8679 0.0003 1.8700 0.0004 −0.9997 0.0012 0.1313 −0.0002 −0.8692), and refined using HKLF 5 procedure of SHELXL. Two of three crystallographically independent F atoms in $[SiF_6]^{2-}$ anion are disordered over two positions with the occupancies of 0.855(9) and 0.145(9). The C– bound H-atoms were placed in calculated positions and were treated using a riding model approximation with U_{iso}(-H) = 1.2 U_{eq}(C), while the N– and O– bound H-atoms were found from differential Fourier maps at intermediate stages of the refinement and their positions were restrained using DFIX instruction. These hydrogen atoms were refined with isotropic displacement parameter U_{iso}(H) = 1.5 U_{eq}(O). The figures were produced using MERCURY [31]. Crystallographic data (cif files) for

I–V, **Vb** have been deposited with the Cambridge Crystallographic Data Center, CCDC Nos. 977655–977660. Copies of this information may be obtained free of charge from The Director, CCDC, 12 Union Road, Cambridge, CB2 1EZ, UK. (Fax: +44 1233 336 033; deposit@ccdc.cam.ac.uk or www: http://www.ccdc.cam.ac.uk.

References

[1] G. Villalba, R.U. Ayres, H. Schroder, J. Ind. Ecol. 11 (2007) 85–101.
[2] Ed.T. Urbansky, Chem. Rev. 102 (2002) 2837–2854.
[3] J.M. Kauffman, J. Am. Physicians Surg. 10 (2005) 38–44.
[4] T. Suge, A. Kawasaki, K. Ishikawa, T. Matsuo, S. Ebisu, Dent. Mater. 24 (2008) 192–198.
[5] T. Suge, A. Kawasaki, K. Ishikawa, T. Matsuo, S. Ebisu, Dent. Mater. 26 (2010) 29–34.
[6] S. Shibata, T. Suge, K. Ishikawa, T. Matsuo, Am. J. Dent. 24 (2011) 148–152.
[7] S. Shibata, T. Suge, T. Kimura, K. Ishikawa, T. Matsuo, Am. J. Dent. 25 (2012) 31–34.
[8] Yu. Hosoya, E. Watanabe, K. Tadokoro, T. Inoue, M. Miyazaki, F.R. Tay, J. Oral Sci. 54 (2012) 267–272.
[9] A. Petrosyan, V. Ghazaryan, M. Fleck, A. Harutyunyan, L. Andriasyan, N. Brsikyan, Armenian patent AM20110068 (2011).
[10] N.A. Brsikyan, L.H. Andriasyan, G.R. Badalyan, A. Harutyunyan, A.M. Petrosyan, V.V. Ghazaryan, New Armenian Med. J. 6 (2012) 52–55.
[11] A. Rosenblatt, T.C.M. Stamford, R. Niederman, J. Dent. Res. 88 (2009) 116–125.
[12] P. Li, K. Nakanishi, T. Kokubo, K. de Groot, Biomaterials 14 (1993) 963–968.
[13] A. Kawasaki, T. Suge, K. Ishikawa, K. Ozaki, T. Matsuo, S. Ebisu, J. Mater. Sci.: Mater. Med. 16 (2005) 461–466.
[14] N. Kurtessis, K. Menzel, G. Weilog, Pat. DDR 92997 (1971).
[15] V.O. Gelmboldt, L.V. Koroeva, Ed.V. Ganin, M.S. Fonari, M.M. Botoshansky, A.A. Ennan, J. Fluorine Chem. 129 (2008) 632–636.
[16] V.O. Gelmboldt, Ed.V. Ganin, M.S. Fonari, L.V. Koroeva, Yu.Ed. Ivanov, M.M. Botoshansky, J. Fluorine Chem. 130 (2009) 428–433.
[17] V.O. Gelmboldt, V.E. Kuz'min, V.Yu. Anisimov, O.V. Prodan, Odes. Med. Zhurnal 135 (2013) 6–10.
[18] D. Adley, P.H. Bird, A.R. Fraser, M. Onyszchuk, Inorg. Chem. 11 (1972) 1402–1409.
[19] V.O. Gelmboldt, Russ. J. Inorg. Chem. 54 (2009) 916–921.
[20] M. Etter, Acc. Chem. Res. 23 (1990) 120–126.
[21] D.G. Golovanov, K.A. Lyssenko, M.Yu. Antipin, Ya.S. Vygodskii, E.I. Lozinskaya, A.S. Shaplov, CrystEngComm 7 (2005) 53–56.
[22] I. Boldog, J.-C. Daran, A.N. Chernega, Ed.B. Rusanov, H. Krautscheid, K.V. Domasevitch, Cryst. Growth Des. 9 (2009) 2895–2905.
[23] A.S. Degtyarenko, Ed.B. Rusanov, A. Bauzá, A. Frontera, H. Krautscheid, A.N. Chernega, A.A. Mokhir, K.V. Domasevitch, Chem. Commun. 49 (2013) 9018–9020.
[24] M.G. Voronkov, L.I. Gubanova, Main Group Met. Chem. 10 (1987) 209–286.
[25] T. Steiner, Angew. Chem. Int. Ed. 41 (2002) 48–76.
[26] A. Pevec, A. Demšar, J. Fluorine Chem. 129 (2008) 707–712.
[27] V.O. Gelmboldt, Russ. J. Inorg. Chem. 57 (2012) 287–291.
[28] C.A. Lipinski, F. Lombardo, B.W. Dominy, P.J. Feeney, Adv. Drug Del. Rev. 46 (2001) 3–26.
[29] W.F. Finney, E. Wilson, A. Callender, M.D. Morris, L.W. Beck, Environ. Sci. Technol. 40 (2006) 2572–2577.
[30] G.M. Sheldrick, Acta Crystallogr. A64 (2008) 112–122.
[31] C.F. Macrae, P.R. Edgington, P. McCabe, E. Pidcock, G.P. Shields, R. Taylor, M. Towler, J. van de Streek, J. Appl. Crystallogr. 39 (2006) 453–457.